Published in final edited form as:
Stem Cells. 2013 January ; 31(1): 23–34. doi:10.1002/stem.1273.

Effective Elimination of Cancer Stem Cells by a Novel Drug Combination Strategy

Shuqiang Yuan[a,b], **Feng Wang**[a,b], **Gang Chen**[b], **Hui Zhang**[b], **Li Feng**[b], **Lei Wang**[c], **Howard Colman**[d], **Michael J. Keating**[e], **Xiaonan Li**[f], **Rui-Hua Xu**[a], **Jianping Wang**[c], and **Peng Huang**[a,b]

[a]State Key Laboratory of Oncology in South China, Sun Yat-sen University Cancer Center, Guangzhou, Guangdong, China

[b]Department of Molecular Pathology, The University of Texas MD Anderson Cancer Center, Houston, Texas, USA

[c]Department of Colorectal Surgery, Sixth Hospital of Sun Yat-sen University, Guangzhou, Guangdong, China

[d]Department of Neuro-Oncology, University of Utah, Salt Lake City, Utah, USA

[e]Department of Leukemia, The University of Texas MD Anderson Cancer Center, Houston, Texas, USA

[f]Department of Molecular and Cellular Biology, Texas Children's Hospital, Baylor College of Medicine, Houston, Texas, USA

Abstract

Development of effective therapeutic strategies to eliminate Cancer stem cells (CSCs), which play a major role in drug resistance and disease recurrence, is critical to improve cancer treatment outcomes. Our study showed that glioblastoma stem cells (GSCs) exhibited low mitochondrial respiration and high glycolytic activity. These GSCs were highly resistant to standard drugs such as carmustine and temozolomide, but showed high sensitivity to a glycolytic inhibitor 3-bromo-2-oxopropionate-1-propyl ester (3-BrOP), especially under hypoxic conditions. We further showed that combination of 3-BrOP with carmustine but not with temozolomide achieved a striking synergistic effect and effectively killed GSCs through a rapid depletion of cellular ATP and inhibition of carmustine-induced DNA repair. This drug combination significantly impaired the sphere formation ability of GSCs *in vitro* and tumor formation *in vivo*, leading to increase in the overall survival of mice bearing orthotopic inoculation of GSCs. Further mechanistic study showed that 3-BrOP and carmustine inhibited glyceraldehyde-3-phosphate dehydrogenase and caused a severe energy crisis in GSCs. Our study suggests that GSCs are highly glycolytic and that certain drug combination strategies can be used to effectively overcome their drug resistance based on their metabolic properties.

Correspondence: Peng Huang, Department of Molecular Pathology, Unit 951, The University of Texas MD Anderson Cancer Center, 1515 Holcombe Blvd., Houston, Texas 77030, USA. Telephone: 713-834-6044; Fax: 713-834-6084; phuang@mdanderson.org.

Author contributions: S.Y.: conception and design, collection/assembly of data, data analysis/interpretation, manuscript writing, final approval; F.W.: conception and design, collection/assembly of data, data analysis/interpretation, manuscript writing, final approval; G.C.: provision of study materials, final approval; H.Z.: provision of study materials, final approval; L.F.: collection/assembly of data; L.W.: provision of study materials, final approval; H.C.: provision of study materials, final approval; M.K.: provision of study materials, final approval; R.X.: provision of study materials, final approval; J.W.: provision of study materials, final approval; X.L.: design of animal study, data analysis/interpretation, P.H.: conception and design, provision of study materials, data analysis/interpretation, final approval. S.Y. and F.W. contributed equally to this article.

Disclosure of Potential Conflicts of Interest

The authors indicate no potential conflicts of interest.

Keywords

Glioma; Hypoxia; Chemotherapy; Drug target; Toxicity

Introduction

Cancer stem cells (CSCs) are a subgroup of cancer cells that have the ability to self-renew, to differentiate into multiple lineage cells, and to initiate tumors *in vivo* [1]. They have been found in hematopoietic malignancies [2] and different types of solid tumors including brain [3], breast [4], colon [5] and pancreatic [6] cancers. A growing body of studies indicates that CSCs are intrinsically more resistant to chemotherapeutic agents and radiation than the bulk of tumor cells, and thus play an important role in persistence of cancer residual disease and recurrence [1]. This drug resistance in CSCs has been attributed to highly expressed drug efflux pumps (such as multidrug resistance proteins), enhanced DNA repair proteins, expression of antiapoptotic proteins, and a slow rate of cell proliferation [1]. Thus, it is important to develop effective therapeutic strategies to eliminate CSCs and overcome cancer resistance to chemotherapy and radiotherapy. However, currently very limited therapeutic strategies are effective in eliminating CSCs, which remains a major challenge in cancer treatment.

Glioblastoma multiforme (GBM), a WHO grade IV astrocytoma, is the most common and aggressive primary brain tumor in adults. Although maximal surgical resection, radiotherapy, and chemotherapy are performed in GBM patients, the treatment outcomes are still dismal, with a median survival of only 12–15 months and the 5-year survival rate of less than 10% [7, 8]. Previous studies demonstrated that glioblastoma stem cells (GSCs) are resistant to conventional chemotherapy drugs carmustine (BCNU) and temozolomide (TMZ) as well as radiation [9, 10]. Since the GSCs are probably responsible for the recurrence of GBM [11–14], how to target the GSCs became a crucial question. The GSCs have been found in the hypoxic niches, which further promote drug resistance [15–17]. Under hypoxic conditions, cancer cells are more dependent on the glycolytic pathway to generate ATP and metabolic intermediates for survival and proliferation. Based on these observations, we postulated that GSCs might be more reliant on glycolysis to maintain their energy homeostasis and stemness than non-stem tumor cells. As such, targeting the glycolytic pathway might be a preferential and effective strategy to kill GSCs.

Development of novel therapeutic agents that target cancer cell metabolism has become an important area of research. Compounds known to inhibit the glycolytic pathway include 2-deoxyglucose and 3-bromopyruvate (3-BrPA) [18–20]. In particular, 3-BrPA is an alkylating agent that has been shown to inhibit hexokinase and glyceraldehyde-3-phosphate dehydrogenase (GAPDH), two key enzymes in the glycolytic pathway [18, 21]. A derivative of 3-BrPA, 3-bromo-2-oxopropionate-1-propyl ester (3-BrOP), is chemically more stable than 3-BrPA and has been shown to be highly potent in causing ATP depletion in cancer cells [22]. In this study, we found that GSCs exhibited low mitochondrial respiration and high glycolytic activity, and further tested the possibility that 3-BrOP might be able to effectively inhibit glycolysis in GSCs and cause severe ATP depletion that might render GSCs incapable of repairing DNA damage induced by chemotherapeutic agents. Using two GSC cell lines, GSC11 and GSC23, which were established from human primary glioblastoma tissues with high expression of a stem cell marker CD133[23], we showed that GSCs were highly sensitive to 3-BrOP, especially under hypoxic conditions, and that combination of this compound with BCNU had striking synergistic effect in eliminating the GSCs.

Materials and Methods

Chemicals and reagents

Carmustine (BCNU), temozolomide (TMZ), and 3-BrPA were purchased from Sigma. 3-BrOP was synthesized by esterification of 3-bromo-2-oxopropionate (Sigma) with 1-propanol (Sigma) as described previously [22].

Cells and cell cultures

GSC11 and GSC23 originally derived from human primary glioblastoma tissues were maintained in DMEM/F-12 (Mediatech) supplemented with B-27 (Invitrogen), 2 mM glutamine (Mediatech), 20 ng/ml recombinant human epidermal growth factor (EGF; R&D Systems), and 20 ng/ml basic fibroblast growth factor (bFGF; R&D Systems) [24]. To induce cancer stem cell differentiation, GSCs were cultured in DMEM/F-12 medium containing 10% FBS for various periods of time as indicated in each experiment. The glioma cell line U87 and non-malignant human astrocytes (NHAs) were maintained in DMEM (Mediatech) supplemented with 10% FBS. Cells were seeded in culture flasks or plates overnight before each treatment. To test the cytotoxic effect of drugs under hypoxic conditions, cells were first pre-incubated in a chamber with 2% oxygen (O_2) and 5% carbon dioxide (CO_2) for 18 h, and then treated with the indicated compounds under the same hypoxic conditions (2% O_2) for the indicated time.

Cell viability assay

Cell-growth inhibition was assayed using a colorimetric assay with MTS (Promega). Briefly, GSCs were seeded in 96-well plates and then treated with indicated compounds at various concentrations. After 72 h incubation, 40 μl MTS solution was added to each well and incubated for another 4 h. The absorbance in each well at 490 nm was measured using a Multiskan plate reader (Thermo Scientific). Cell apoptosis and necrosis were measured using flow cytometric analysis of cells double-stained with FITC-annexin-V and propidium iodide (PI). Briefly, samples were collected, dissociated, washed with cold PBS, and suspended in the annexin-V binding buffer. The cells were stained with annexin-V for 15 minutes at room temperature, washed, and stained with PI. The samples were analyzed using a FACSCalibur flow cytometer equipped with the CellQuest Pro software program (Becton-Dickinson). Cell growth was also confirmed by cell counting using a Coulter Counter (Beckman, Brea, CA, USA). All metabolic parameters (O_2 consumption, glucose uptake, lactate production, ATP depletion, GAPDH and hexokinase activity) were assessed prior to cell death and the results were normalized by cell number.

Tumor sphere forming assay

GSCs were treated with indicated compounds for 3 h and then seeded in fresh medium in 96-well plates in a range of 10–1000 cells per well; neurospheres were counted under a microscope (Nikon) after 3 weeks of incubations.

Tumorigenicity in orthtopic mouse model

All animal experiments were conducted at Baylor College of Medicine according to an Institutional Animal Care and Use Committee-approved protocol. The Rag2/severe complex immune deficiency (SCID) mice, ages 8 to 12 weeks, were bred and maintained in a specific pathogen- free animal facility. GSC11 cells were cultured in GSC medium and made into single cells by Accutase. The same number of GSC11 cells were exposed to PBS, 20μM BCNU, 20μM 3-BrOP or 20μM BCNU plus 20μM 3-BrOP in GSC medium at 37°C for 6 hours, then cells were collected, washed and suspended in serum-free culture medium. After mice were anesthetized with sodium pentobarbital (50mg/kg), GSC11 cells were inoculated

into Rag2/SCID mice cerebral hemisphere (1 mm to the right of the midline, 1.5 mm anterior to the lambdoid suture, and 3 mm deep) at 2×10^5 cells/mouse via a 10-mL 26-gauge Hamilton Gastight 1701 syringe needle. The animals were monitored daily without further drug treatment until they developed signs of neurological deficit or became moribund, at which time they were euthanized [25].

Glucose uptake assay

To compare glucose uptake by GSCs and the serum-induced differentiated GSCs (10% FBS, 20 days), the old culture medium was removed from the respective cell culture, and the cells were incubated in glucose-free, serum-free medium for 2 h at 37°C and then incubated with [^{3}H]2-deoxyglucose (0.4 μ, Ci/ml) for 60 min. After washing with cold PBS, each sample was suspended in 0.5 ml of water and transferred to a vial with 3 ml of scintillation fluid. The radioactivity was detected using a liquid scintillation machine (Beckman Coulter).

Oxygen consumption assay

To compare oxygen consumption by GSCs and the serum-induced differentiated GSCs (10% FBS, 20 days), the old cell culture medium was removed from the respective samples, and the cells were harvested and resuspended in warm serum-free medium pre-equilibrated with 21% oxygen. The cells (7×10^6 cells/ml) were placed in a sealed respiration chamber equipped with a thermostat control and microstirring device (Oxytherm; Hansatech Instruments, Norfolk, UK). Oxygen consumption by the cells in the chamber was measured and constantly monitored at 37°C using a Clark-type oxygen electrode, and was expressed as nanomoles of O_2 consumed as a function of time (nmol/ml/minute).

Lactate production assay

To measure the lactate production by GSCs and the serum-induced differentiated GSCs (10% FBS, 20 days), cells were plated in 6-well plates and cultured in their respective medium for the indicated time. Aliquots of the culture medium were analyzed using the Accutrend lactate analyzer (Roche). To measure the effect of drug treatment on lactate production in short-term culture, cells were plated in 96-well plates and treated with the indicated compounds for 3 h. A colorimetric lactate assay kit was used according to the manufacturer's protocol (Eton Bioscience). Absorbance in each well at 490 nm was measured using a Multiskan plate reader.

ATP depletion assay

GSCs were plated in 96-well plates and treated with the indicated compounds for 3 or 6 h, 100 μl of mixed CellTiter-Glo luminescent reagent (Promega) was then added to each well and incubated for 10 minutes on an orbital shaker. Luminescence was measured using a Fluoroskan luminescence scanner (Thermo Scientific).

Single-cell gel electrophoresis assay (Comet assay)

After GSCs were treated with the indicated compounds for 3 h, cell suspensions mixed with 0.5% low-melting-point agar was placed onto a 24 × 50-mm slide precoated with 1% regular agar. After the agar was solidified, slides were soaked in a prechilled fresh lysing solution (2.5 M NaCl, 100 mM ethylenediaminetetraacetic acid, 10 mM Tris-HCl, 1% Triton X-100, pH 10) for 1 h at 4°C. After rinsing with 0.4 M Tris buffer (pH 7.5), slides were placed in a reservoir filled with fresh electrophoresis buffer (300 mM NaOH, 1 mM ethylenediaminetetraacetic acid, pH>13) for 15 minutes and then subjected to electrophoresis for another 15 minutes (25 V, 300 mA). Slides were then stained with CYBR Green I (Trevigen) and photographed under a fluorescent microscope (Nikon). The

percentage of tail DNA, which indicates damaged DNA, was analyzed using the Casp software program (version 1.2.2) provided by the CASPLab Comet Assay Project.

Western blotting

Cellular proteins were separated using electrophoresis on 10% SDS-PAGE, transferred to nitrocellulose membranes, and then blotted with specific primary antibodies against H_2AX, γH_2AX (Upstate) and β-actin. The bound primary antibodies were detected using appropriate horseradish peroxidase-conjugated secondary antibodies, and the signals were detected using a SuperSignal enhanced chemiluminescence kit (Pierce).

GAPDH enzymatic activity assay

Purified GAPDH enzyme from rabbit muscle (Sigma) or protein extracts prepared from GSC11 cells were used in the GAPDH assays *in vitro*, using a GAPDH Assay Kit (ScienCell) according to the manufacturer's protocol. Purified GAPDH was incubated *in vitro* with the indicated compounds (BCNU, 3-BrOP) for 30 minutes, then added to a mixture of 6.67 mM 3-phosphoglyceric acid, 3.33 mM L-cysteine, 117 μM β-NADH, 1.13 mM ATP, 3.33 U/ml 3-phosphoglycerate kinase, and 100 mM triethanolamine buffer (pH 7.6). The change in NADH fluorescence was then monitored using a Fluoroskan spectrometer every minute for up to 20 minutes. For analysis of GAPDH activity in cell extracts, GSC11 cells were first incubated with or without 3-BrOP, BCNU, or their combination for 30 min, and protein lysates were prepared and immediately used for GAPDH activity assay without addition of 3-BrOP or BCNU *in vitro*.

Hexokinase enzymatic activity assay

Lysates of GSCs pretreated with the indicated compound or purified hexokinase II enzyme from *Saccharomyces cerevisiae* (Sigma-Aldrich) were prepared as described in GAPDH enzymatic activity assay, and added to a mixture of 6.5 mM $MgCl_2$, 220 mM glucose, 2.7 mM ATP, 0.83 mM β-NAD, 0.24 U/ml glucose-6-phosphate dehydrogenase (Sigma-Aldrich), and 100 mM triethanolamine buffer (pH 7.6). Increases in NADH fluorescence were measured using a Fluoroskan fluorescence scanner every 1 minute for up to 20 minutes.

Statistical analysis

Data were analyzed using GraphPad Prism 5 (GraphPad Software). Data graphed with error bars represent mean and SEM from experiments done in triplicate unless otherwise noted. A two-sided Student's t test was used to determine the significance of difference between samples. Survival curves were compared between different groups by Log-rank test.

Results

GSCs Exhibit Low Mitochondrial Respiration and Are Resistant to TMZ and BCNU but Sensitive to Glycolytic Inhibition

Two human glioblastoma stem cell lines, GSC11 and GSC23 were used in this study. Under stem cell culture conditions in serum-free medium, GSC11 cells exhibited typical neurosphere morphology with high expression of neural stem cell marker nestin (Fig 1A), and showed relatively low mitochondrial respiration as evidenced by a low oxygen consumption rate (Fig. 1B). When GSCs were induced to undergo differentiation by exposure to serum [26, 27], the cells gradually lost their neurosphere morphology in medium containing 10% FBS, became attached to the culture dish as a monolayer, and exhibited a substantial decrease in nestin expression (Fig 1A). Associated with this serum-induced differentiation phenotype, there were also a decrease in other glioma stem markers such as

CD133, SOX2, and Notch1 (data not shown). Interestingly, mitochondrial respiration was substantially activated leading to approximately 75% increase in oxygen consumption (Figs. 1B-1C), accompanied by significant decreases in lactate production (Fig. 1D) and a significant decrease in glycolytic index (Fig. 1E). A similar change in energy metabolism (decrease in glycolytic index) was also observed in GSC23 cells induced by serum (Fig 1E). Interestingly, the glycolytic index of the "regular" GBM cells (U87) was also lower than that of GSCs in stem cell medium (Fig 1E), suggesting that although regular cancer cells (non-stem) are generally considered active in glycolysis, cancer stem cells GSCs exhibit even higher glycolytic activity with lower mitochondrial respiration, and serum induction activated mitochondrial function and reduced glycolysis.

When GSC11 cells were incubated with TMZ and BCNU (two drugs commonly used in the treatment of glioblastoma) for 72 h, the cells showed resistance to these conventional chemotherapeutic drugs, especially under hypoxic conditions (Fig. 1F). In contrast, GSCs were more sensitive to 3-BrOP under hypoxic conditions, with the 50% inhibitory concentration of 10~15 μM compared with 20~30 μM under normoxic conditions.

Combination of 3-BrOP and BCNU Shows Synergistic Effect in Killing GSCs, Especially under Hypoxic Conditions

We then tested if a combination of 3-BrOP with BCNU or TMZ could lead to more effective killing of GSCs, based on the rationale that 3-BrOP would deplete the cellular ATP by inhibiting glycolysis and thus impair the ability of cells to repair DNA damage induced by BCNU or TMZ. The results of MTS assay showed that 3-BrOP substantially potentiates the cytotoxic effect of BCNU but not that of TMZ, especially under hypoxic conditions (Figs. 2A-2B). We further confirmed the synergistic killing effect of the 3-BrOP and BCNU combination, using flow cytometry analysis after the cells were double stained with annexin-V/PI. Most GSC11 cells were killed after 24 h treatment with 200 μM BCNU in combination with 15 μM 3-BrOP, whereas we did not observe significant cell death when cells were treated with either drug alone (Fig. 2C). The low cytotoxicity of 15 μM 3-BrOP measured by annexin-V/PI assay was likely due to the relatively short drug incubation time (24 h, compared to 72 h in MTS assay). Similar synergistic drug combination effect was also observed in GSC23 cells (data not shown). Furthermore, greater synergistic effect of BCNU and 3-BrOP was observed in hypoxia than in normoxia, as GSCs were more dependent on glycolysis for ATP generation under hypoxia. Quantitative analysis of the drug combination index (CI) further confirmed the synergism of 3-BrOP and BCNU treatments in GSCs under hypoxia, where the CI values were from 0.701~0.979 (Fig. 2D), indicating the two compounds were synergistic under most combination conditions (CI<1, synergism; CI=1, additive; CI>1, antagonism). This finding suggests that 3-BrOP could be an effective therapeutic agent to target GSCs especially in hypoxic tissue environments.

Combination of 3-BrOP and BCNU Significantly Impairs GSCs' Sphere Formation Ability in vitro and Tumorigenecity in vivo

Since *in vitro* clonogenicity is considered as an indicator of the tumor-initiating capability of cancer cells *in vivo*, we tested the effect of BCNU and 3-BrOP on the ability of GSCs to form colonies of neurospheres. As shown in Figs. 3A-3B, the neurosphere-formation capacity of GSCs decreased slightly when treated with a relatively low concentration of BCNU (50 μM) or 3-BrOP (15 μM) alone. However, combination of both compounds almost completely abolished the neurosphere formation. These results indicate that GSCs underwent irreversible cell death and lost their self-renewal ability even after a short-term treatment with a combination of BCNU and 3-BrOP.

We then further tested the effect of 3-BrOP and BCNU on tumor formation *in vivo* by orthotopic inoculation of GSCs into the brains of the immuno-deficient mice. GSC11 cells were cultured in serum-free medium and treated with PBS (control), 20μM of 3-BrOP, 20μM of BCNU, or their combination for 6 hours, and then inoculated into the mouse brains. Mouse survival was monitored as an indication of in vivo tumor formation and disease progression. All mice in the control died within 80 days, while all mice in the 3-BrOP- or BCNU-treated groups died with a substantial delay, especially in the 3-BrOP-treat group (Fig. 3C), suggesting the drug treatment partially suppress tumor development. Importantly, only two out of the five mice in the drug combination group died by 12 months, and the remaining 3 mice exhibited no signs of tumor development (Fig. 3C), suggesting that this drug combination significantly impaired the tumorigenesis of GSCs (P=0.0027).

3-BrOP in Combination with BCNU Preferentially Kills Tumor Cells with Relatively Low Toxic Effect on Non-malignant Human Astrocytes (NHAs)

Since cancer cells, especially GSCs, are more dependent on glycolytic pathway to generate ATP, we hypothesized that inhibition of glycolysis by 3-BrOP would preferentially deplete ATP in GSCs and other cancer cells, but the non-malignant cells such as NHAs would be less sensitive to such inhibition. Indeed, as shown in Fig. 4a combination of sub-toxic concentrations of 3-BrOP (15 μM) and BCNU (200 μM) synergistically killed most of GSC11 (Fig. 2C) and GSC23 cells (Fig. 4A). Higher concentration of 3-BrOP (20 μM) was needed to achieve similar killing effect in the serum-induced GSC11 and GSC23 cells (Fig. 4B and Supplementary Fig. S1). We also noted that a higher concentration (30 μM) of 3-BrOP was needed to cause similar killing effect in U87 cells (Fig. 4D) compared to GSC11 or GSC23 cells (15 μM), suggesting that the GSCs are more sensitive to the combination of 3-BrOP and BCNU. Importantly, this drug combination caused only minimum cytotoxicity in the immortalized normal human astrocytes (NHAs, Fig. 4C). These observations suggest that normal human cells may be fundamentally different from malignant cells in their energy metabolism and sensitivity to glycolytic inhibitor, which thus may provide a therapeutic window for selectivity. Interestingly, NHA cells and U87 cells exhibited similar doubling-times but had different drug sensitivity, while serum-induction of differentiation moderately increased the doubling-times of glioma stem cells (Supplementary Fig. S2) and decreased their drug sensitivity.

Severe Depletion of Cellular ATP by 3-BrOP and BCNU in GSCs Prior to Cell Death

We then tested the effect of 3-BrOP or its combination with BCNU on glycolysis in GSCs, using lactate production as an indicator of glycolytic activity. As shown in Fig. 5A, a 3 hour incubation of GSC11 cells with 100–200 μM BCNU or 15–20 μM 3-BrOP alone caused only a slight inhibition of lactate production. However, the combination of these two compounds showed a significant inhibition of lactate (Fig. 5A), leading to a substantial decrease of cellular ATP by more than 50% (Fig. 5B). A prolonged incubation with both compounds for 6 hours in hypoxia led to significant depletion of ATP, although incubation with 200 μM BCNU or 15 μM 3-BrOP alone caused only a slight reduction of ATP (Fig. 5C). Similar effect of 3-BrOP and BCNU in causing lactate production inhibition (data not shown) and ATP depletion (Fig. 5D) was also observed in GSC23 cells. In contrast, treatment of GSCs with TMZ alone did not cause a significant change of ATP in GSC11 or GSC23 cells, and this compound was unable to enhance the ability of 3-BrOP to cause further depletion of ATP in GSCs (Fig. 5E & 5F). This might explain why treatment of GSCs with 3-BrOP plus TMZ did not show any enhancement of cytotoxicity. Flow cytometry analysis of cell viability showed that GSCs treated with 3-BrOP plus BCNU remained largely viable at both the 3 hour and 6 hour time points, suggesting that the observed ATP depletion was an early event and was not a consequence of cell death (Fig. 5G).

Effect of BCNU and 3-BrOP on the enzyme activity of GAPDH and HK

The observation that BCNU but not TMZ was able to potentiate the ability of 3-BrOP to deplete ATP led us to speculate that BCNU might have certain unique mechanism of action different from TMZ. Since BCNU is known to inhibit glutathione reductase by alkylating its thiolate-active site [28], we postulated that it is possible that this compound might inhibit the glycolytic enzyme GAPDH, which also has potential thiolate-active site. To test this possibility, we measured GAPDH activity in GSCs before and after treatment with BCNU or 3-BrOP alone or in combination for 30 minutes. Interestingly, treatment with 10 μM 3-BrOP or 200 μM BCNU alone inhibited GAPDH activity by about 60% (Fig. 6A), and treatment with the combination of the two compounds inhibited GAPDH activity by almost 80%, which may explain why ATP was severely depleted in the combination setting. We further confirmed the inhibition of purified GAPDH by BCNU and 3-BrOP at various concentrations using an *in vitro* enzymatic assay. The concentrations of BCNU and 3-BrOP required to inhibit the purified GAPDH activity by 50% were about 200 μM and 10 μM, respectively (Figs. 6B and 6C). Incubation of purified GAPDH with the combination of BCNU and 3-BrOP *in vitro* resulted in further inhibition of GAPDH activity (Fig. 6D). Interestingly, 3-BrOP (10 μM) and BCNU (100–200 μM) at the concentrations that inhibited GAPDH activity did not showed significant inhibitory effect on hexokinase activity in GSC11 cells (Fig. 6E), suggesting that at the low drug concentrations, the main enzyme target was GAPDH not hexokinase. We also performed in vitro assays using purified hexokinase II and confirmed that 3-BrOP at the concentrations of 3–100 μM did not inhibit hexokinase activity, while a higher concentration (300 μM) slightly inhibited HKII in vitro (Fig. 6F).

3-BrOP Impairs the Ability of GSCs to Repair BCNU-Induced DNA Damage

BCNU can cause DNA damage by formation of DNA adducts and also cause inter-strand cross-links and double-strand breaks (DSBs) in DNA [29, 30]. DSBs are repaired in mammalian cells by nonhomologous end-joining and homologous recombination repair [31], in which formation of γH$_2$AX foci is a rapid cellular response to the presence of DSBs [32]. Because ATP is required for H$_2$AX phosphorylation and the subsequent complicated DNA repair process, we speculated that depletion of ATP in GSC cells by 3-BrOP would compromise the DNA repair. Using a comet assay, we observed that treatment with BCNU alone or combination with 3-BrOP for 6 h caused severe DNA damage in GSCs, resulting in the appearance of broken DNA as the comet tails after single-cell gel electrophoresis (Figs. 7A and 7B). In GSCs treated with BCNU alone, the DNA damage could be repaired 3–6 h after the removal of BCNU, as evidenced by the disappearance or reduction of the DNA tails (Figs. 7A and 7B). However, the GSCs were unable to repair the DNA damage when treated with a combination of BCNU and 3-BrOP (Fig. 7A). In fact, the percentage of DNA in the tails increased from 50% to 60% after a 3 hour recovery and to more than 80% after 6 hour in GSCs treated with the drug combination. Using flow cytometry, we confirmed that the cell death in the combination treatment was irreversible even after 18 hour of recovery in fresh medium (Fig. 7A, lower panel).

Immediately after formation of DSBs, the MRN complex (MRE11, RAD50, and NBS1) binds to broken DNA ends and recruits ATM (ataxia telangiectasia, mutated), ATR (ATM- and Rad3-related), and/or DNA-dependent protein kinase, resulting in phosphorylation of H$_2$AX (γH$_2$AX) and initiation of the DNA-repair process [33], and dephosphorylation and removal of γH$_2$AX in the cancer cells is a step toward turning off the DNA damage response [34]. In our study, we observed that when GSCs were incubated with BCNU for 4 h alone or in combination with 3-BrOP induced a substantial increase in γH$_2$AX. When we continuously treated GSCs for 6 h, we observed that γH$_2$AX was present in the BCNU-treated cells (Fig. 7C), indicating DNA damage and active repair were ongoing. However, in

cells treated with 3-BrOP or its combination with BCNU for 6 h, γH_2AX decreased substantially (Fig. 7C), suggesting a dephosphorylation of H_2AX due to a lack of ATP to support the DNA repair process.

DISCUSSION

In the present study, we showed that GSCs had low mitochondrial respiration and high glycolytic activity, which may serve as a biochemical basis for developing novel therapeutic strategies to effectively target GSCs using a rational drug combination. The biochemical mechanism-based drug combination of an effective glycolytic inhibitor 3-BrOP and a conventional chemotherapeutic agent BCNU exhibited a striking synergistic killing effect in GSCs. Almost all GSCs were killed by this combination in 24 h. This finding raises a potential for use of this drug combination to eliminate GSCs and overcome the resistance of glioblastoma to existing chemotherapeutic agents, especially under hypoxic conditions.

Patients with glioblastoma multiforme have poor prognosis, and there have been only limited improvements of therapeutic outcomes during the past two decades [35]. GSCs seem to reside in the niches where the cells are in hypoxic microenvironment, which contributes significantly to cancer chemoresistance and radioresistance [1]. Although an increase in drug dosage could increase the effective drug concentration in the brain to kill more cancer cells, this may also increase toxic side effect and thus limit its applications. Furthermore, GSCs may adapt quickly to drug treatment by up-regulating the expression of drug efflux pumps, anti-apoptotic proteins, and DNA repair proteins like O^6-methylguanine-DNA methyltransferase. In the case of BCNU, this compound has a very short half-life and the drug become undetectable after 5 minutes of treatment [36]. BCNU penetration in the brain tissue occurs over only a very short distance, approximately 2 mm from the ependymal surface [37]. Thus, achieving and maintaining effective high concentration of BCNU in the tumor tissue is difficult. For effective and selective killing of cancer cells, especially CSCs, determining the fundamental differences between cancer and normal cells is critically important. Energy metabolism has emerged as a potential candidate target for treatment of cancers. Multiple studies have confirmed that nutrient metabolism in cancer cells may be different from that in normal cells. As first proposed by Otto Warburg [38], cancer cells might rely more on glycolysis for metabolism and survival due in part to mitochondrial dysfunction.

In the present study, we observed that mitochondrial respiratory activity was down-regulated in GSCs, and glycolysis seem to be a major energy source to maintain their survival. An effective agent that targets glycolysis can achieve the goal of eliminating CSCs. We postulated that ATP depletion induced by glycolytic inhibition could cause a severe energy crisis, which could lead to a severe compromise of GSC's ability to repair DNA damage induced by chemotherapeutic agents. However, it seems necessary to deplete ATP to certain level in order to effectively compromise the ability of DNA repair. In GSCs, this severe ATP depletion could be efficiently achieved by combination of 3-BrOP with BCNU, but not with TMZ. This seems due to the ability of BCNU and 3-BrOP to inhibit GAPDH activity in a synergistic fashion. Although hexokinase has been considered a major target of 3-bromopyruvate [19, 39–41], high concentrations are needed to inhibit this enzyme. A recent study using HepG2 cells suggested that this 3-bromopyruvate might inhibit GAPDH more effectively [42]. Our study showed that 3-BrOP at low concentrations preferentially inhibited GAPDH in GSCs without significant effect on hexokinase. It should be noted, however, that inhibiton of hexokinase can still be a feasible strategy to impact cancer energy metabolism for therapeutic purpose. Interestingly, a recent study show that suppression of hexokinase II by siRNA causes a decrease in glycolysis and a restoration of oxidative phosphorylation, leading to sensitization to TMZ treatment [43].

The observation that BCNU inhibited GAPDH activity is a novel finding in study. The primary pharmacological action of BCNU has been traditionally attributed to its alkylating activity that inhibits DNA synthesis and repair mediated by its active chloroethyl moieties [44]. BCNU is also known to inhibit glutathione reductase and thioredoxin reductase by alkylating its thiolate-active site[45]. Similar to glutathione reductase, GAPDH contains many thiol groups that can be alkylated. GAPDH activity in cancer cells can be inactivated by a number of covalent modifications, including S-nitrosylation of the protein thiols [46], disulfide formation [46], covalent binding of NAD^+ through a nitric oxide (NO)-dependent thiol intermediate [47] and mono(ADP-ribosyl)ation [48]. BCNU may covalently inactivate GAPDH activity by S-nitrosylation of cysteine thiols. It is interesting to note that although GAPDH activity could be inhibited by 50% with 200 μM BCNU *in vitro* using a direct enzyme assay, we observed only a moderate decrease in cellular ATP after a 6-h treatment of GSCs with 200 μM BCNU alone. A possible explanation for the only modest ATP decrease could be that BCNU might be less effective in inhibiting GAPDH in intact cells, and that the moderate inhibition of glycolysis by BCNU might have been compensated by mitochondrial oxidative phosphorylation. This is in contrast to 3-BrOP, which seems to inhibit both glycolysis and mitochondrial respiration [42, 49, 50]. This might explain why 3-BrOP could deplete ATP more efficiently than BCNU when each compound was used alone. The combination of sub-toxic concentrations of 3-BrOP and BCNU seems to be an effective way to inhibit GAPDH and to achieve optimal killing of GSCs with low toxicity to normal cells. This is largely due to the unique mechanisms of action of each compound and the biological properties of glioblastoma stem cells, which are highly dependent on glycolysis and thus sensitive to such metabolic intervention. The ability of 3-BrOP and BCNU combination to effectively eliminate cancer stem cells in vitro and impair their tumor formation in vivo suggest that this novel drug combination merits further evaluation for their potential to be used in cancer treatment.

CONCLUSION

3-BrOP, a novel effective glycolytic inhibitor, can effectively sensitize GSCs to the killing effect of BCNU, resulting in striking synergistic elimination of these cells *in vitro* and suppression of tumor formation *in vivo*. 3-BrOP is a promising drug that preferentially targets cancer cells, especially CSCs in hypoxic environment. Combination of 3-BrOP and BCNU merits further evaluation in pre-clinical and clinical setting for potential treatment of glioblastoma.

Supplementary Material

Refer to Web version on PubMed Central for supplementary material.

Acknowledgments

We thank Dr. Howard Colman for providing GSC11 and GSC23 cells. We thank Dr. Xiao-nan Li for providing assistance in animal study. This work was supported in part by grants CA085563, CA100428, and CA16672 from the National Institutes of Health, and a grant for the CLL Global Research Foundation. Feng Wang was supported by the Rosalie B Hite Fellowship from MD Anderson Cancer Center.

This work was supported in part by grants CA085563, CA100428, and CA16672 from the National Institutes of Health, and a grant for the CLL Global Research Foundation. Feng Wang was supported by the Rosalie B Hite Fellowship from MD Anderson Cancer Center.

References

1. Gilbert CA, Ross AH. Cancer stem cells: cell culture, markers, and targets for new therapies. J Cell Biochem. 2009; 108:1031–1038. [PubMed: 19760641]

2. Bonnet D, Dick JE. Human acute myeloid leukemia is organized as a hierarchy that originates from a primitive hematopoietic cell. Nat Med. 1997; 3:730–737. [PubMed: 9212098]
3. Singh SK, Clarke ID, Terasaki M, et al. Identification of a cancer stem cell in human brain tumors. Cancer Res. 2003; 63:5821–5828. [PubMed: 14522905]
4. Al-Hajj M, Wicha MS, Benito-Hernandez A, et al. Prospective identification of tumorigenic breast cancer cells. Proc Natl Acad Sci U S A. 2003; 100:3983–3988. [PubMed: 12629218]
5. O'Brien CA, Pollett A, Gallinger S, et al. A human colon cancer cell capable of initiating tumour growth in immunodeficient mice. Nature. 2007; 445:106–110. [PubMed: 17122772]
6. Li C, Heidt DG, Dalerba P, et al. Identification of pancreatic cancer stem cells. Cancer Res. 2007; 67:1030–1037. [PubMed: 17283135]
7. Stupp R, Mason WP, van den Bent MJ, et al. Radiotherapy plus concomitant and adjuvant temozolomide for glioblastoma. N Engl J Med. 2005; 352:987–996. [PubMed: 15758009]
8. Stupp R, Hegi ME, Mason WP, et al. Effects of radiotherapy with concomitant and adjuvant temozolomide versus radiotherapy alone on survival in glioblastoma in a randomised phase III study: 5-year analysis of the EORTC-NCIC trial. Lancet Oncol. 2009; 10:459–466. [PubMed: 19269895]
9. Kang MK, Kang SK. Tumorigenesis of chemotherapeutic drug-resistant cancer stem-like cells in brain glioma. Stem Cells Dev. 2007; 16:837–847. [PubMed: 17999604]
10. Beier D, Schulz JB, Beier CP. Chemoresistance of glioblastoma cancer stem cells--much more complex than expected. Mol Cancer. 10:128. [PubMed: 21988793]
11. Bao S, Wu Q, McLendon RE, et al. Glioma stem cells promote radioresistance by preferential activation of the DNA damage response. Nature. 2006; 444:756–760. [PubMed: 17051156]
12. Johannessen TC, Wang J, Skaftnesmo KO, et al. Highly infiltrative brain tumours show reduced chemosensitivity associated with a stem cell-like phenotype. Neuropathol Appl Neurobiol. 2009; 35:380–393. [PubMed: 19508445]
13. Liu G, Yuan X, Zeng Z, et al. Analysis of gene expression and chemoresistance of CD133+ cancer stem cells in glioblastoma. Mol Cancer. 2006; 5:67. [PubMed: 17140455]
14. Chekenya M, Krakstad C, Svendsen A, et al. The progenitor cell marker NG2/MPG promotes chemoresistance by activation of integrin-dependent PI3K/Akt signaling. Oncogene. 2008; 27:5182–5194. [PubMed: 18469852]
15. Lei Z, Li B, Yang Z, et al. Regulation of HIF-1alpha and VEGF by miR-20b tunes tumor cells to adapt to the alteration of oxygen concentration. PLoS One. 2009; 4:e7629. [PubMed: 19893619]
16. Heddleston JM, Li Z, McLendon RE, et al. The hypoxic microenvironment maintains glioblastoma stem cells and promotes reprogramming towards a cancer stem cell phenotype. Cell Cycle. 2009; 8:3274–3284. [PubMed: 19770585]
17. Li Z, Bao S, Wu Q, et al. Hypoxia-inducible factors regulate tumorigenic capacity of glioma stem cells. Cancer Cell. 2009; 15:501–513. [PubMed: 19477429]
18. Ko YH, Pedersen PL, Geschwind JF. Glucose catabolism in the rabbit VX2 tumor model for liver cancer: characterization and targeting hexokinase. Cancer Lett. 2001; 173:83–91. [PubMed: 11578813]
19. Geschwind JF, Ko YH, Torbenson MS, et al. Novel therapy for liver cancer: direct intraarterial injection of a potent inhibitor of ATP production. Cancer Res. 2002; 62:3909–3913. [PubMed: 12124317]
20. Nelson K. 3-Bromopyruvate kills cancer cells in animals. Lancet Oncol. 2002; 3:524. [PubMed: 12217784]
21. Geschwind JF, Georgiades CS, Ko YH, et al. Recently elucidated energy catabolism pathways provide opportunities for novel treatments in hepatocellular carcinoma. Expert Rev Anticancer Ther. 2004; 4:449–457. [PubMed: 15161443]
22. Xu RH, Pelicano H, Zhang H, et al. Synergistic effect of targeting mTOR by rapamycin and depleting ATP by inhibition of glycolysis in lymphoma and leukemia cells. Leukemia. 2005; 19:2153–2158. [PubMed: 16193082]
23. Jiang H, Gomez-Manzano C, Aoki H, et al. Examination of the therapeutic potential of Delta-24-RGD in brain tumor stem cells: role of autophagic cell death. J Natl Cancer Inst. 2007; 99:1410–1414. [PubMed: 17848677]

24. Lee J, Kotliarova S, Kotliarov Y, et al. Tumor stem cells derived from glioblastomas cultured in bFGF and EGF more closely mirror the phenotype and genotype of primary tumors than do serum-cultured cell lines. Cancer Cell. 2006; 9:391–403. [PubMed: 16697959]
25. Yu L, Baxter PA, Voicu H, et al. A clinically relevant orthotopic xenograft model of ependymoma that maintains the genomic signature of the primary tumor and preserves cancer stem cells in vivo. Neuro Oncol. 2010; 12:580–594. [PubMed: 20511191]
26. Rieske P, Golanska E, Zakrzewska M, et al. Arrested neural and advanced mesenchymal differentiation of glioblastoma cells-comparative study with neural progenitors. BMC Cancer. 2009; 9:54. [PubMed: 19216795]
27. He H, Nilsson CL, Emmett MR, et al. Glycomic and transcriptomic response of GSC11 glioblastoma stem cells to STAT3 phosphorylation inhibition and serum-induced differentiation. J Proteome Res. 2010; 9:2098–2108. [PubMed: 20199106]
28. Schallreuter KU, Gleason FK, Wood JM. The mechanism of action of the nitrosourea anti-tumor drugs on thioredoxin reductase, glutathione reductase and ribonucleotide reductase. Biochim Biophys Acta. 1990; 1054:14–20. [PubMed: 2200526]
29. Batista LF, Roos WP, Christmann M, et al. Differential sensitivity of malignant glioma cells to methylating and chloroethylating anticancer drugs: p53 determines the switch by regulating, xpc, ddb2, and DNA double-strand breaks. Cancer Res. 2007; 67:11886–11895. [PubMed: 18089819]
30. Cui B, Johnson SP, Bullock N, et al. Bifunctional DNA alkylator 1,3-bis(2-chloroethyl)-1-nitrosourea activates the ATR-Chk1 pathway independently of the mismatch repair pathway. Mol Pharmacol. 2009; 75:1356–1363. [PubMed: 19261750]
31. Drablos F, Feyzi E, Aas PA, et al. Alkylation damage in DNA and RNA--repair mechanisms and medical significance. DNA Repair (Amst). 2004; 3:1389–1407. [PubMed: 15380096]
32. Rogakou EP, Pilch DR, Orr AH, et al. DNA double-stranded breaks induce histone H2AX phosphorylation on serine 139. J Biol Chem. 1998; 273:5858–5868. [PubMed: 9488723]
33. Ikura T, Tashiro S, Kakino A, et al. DNA damage-dependent acetylation and ubiquitination of H2AX enhances chromatin dynamics. Mol Cell Biol. 2007; 27:7028–7040. [PubMed: 17709392]
34. Rai R, Peng G, Li K, et al. DNA damage response: the players, the network and the role in tumor suppression. Cancer Genomics Proteomics. 2007; 4:99–106. [PubMed: 17804872]
35. Ohgaki H, Kleihues P. Population-based studies on incidence, survival rates, and genetic alterations in astrocytic and oligodendroglial gliomas. J Neuropathol Exp Neurol. 2005; 64:479–489. [PubMed: 15977639]
36. Oliverio VT. Pharmacology of the nitrosoureas: an overview. Cancer Treat Rep. 1976; 60:703–707. [PubMed: 821608]
37. Blasberg RG, Patlak C, Fenstermacher JD. Intrathecal chemotherapy: brain tissue profiles after ventriculocisternal perfusion. J Pharmacol Exp Ther. 1975; 195:73–83. [PubMed: 810575]
38. Warburg O. On the origin of cancer cells. Science. 1956; 123:309–314. [PubMed: 13298683]
39. Ko YH, Smith BL, Wang Y, et al. Advanced cancers: eradication in all cases using 3-bromopyruvate therapy to deplete ATP. Biochem Biophys Res Commun. 2004; 324:269–275. [PubMed: 15465013]
40. Xu RH, Pelicano H, Zhou Y, et al. Inhibition of glycolysis in cancer cells: a novel strategy to overcome drug resistance associated with mitochondrial respiratory defect and hypoxia. Cancer Res. 2005; 65:613–621. [PubMed: 15695406]
41. Chen Z, Zhang H, Lu W, et al. Role of mitochondria-associated hexokinase II in cancer cell death induced by 3-bromopyruvate. Biochim Biophys Acta. 2009; 1787:553–560. [PubMed: 19285479]
42. Pereira da Silva AP, El-Bacha T, Kyaw N, et al. Inhibition of energy-producing pathways of HepG2 cells by 3-bromopyruvate. Biochem J. 2009; 417:717–726. [PubMed: 18945211]
43. Wolf A, Agnihotri S, Micallef J, et al. Hexokinase 2 is a key mediator of aerobic glycolysis and promotes tumor growth in human glioblastoma multiforme. J Exp Med. 2011; 208:313–326. [PubMed: 21242296]
44. Woolley PV, Dion RL, Kohn KW, et al. Binding of 1-(2-chloroethyl)-3-cyclohexyl-1-nitrosourea to L1210 cell nuclear proteins. Cancer Res. 1976; 36:1470–1474. [PubMed: 4221]

45. Witte AB, Anestal K, Jerremalm E, et al. Inhibition of thioredoxin reductase but not of glutathione reductase by the major classes of alkylating and platinum-containing anticancer compounds. Free Radic Biol Med. 2005; 39:696–703. [PubMed: 16085187]

46. Molina y Vedia L, McDonald B, Reep B, et al. Nitric oxide-induced S-nitrosylation of glyceraldehyde-3-phosphate dehydrogenase inhibits enzymatic activity and increases endogenous ADP-ribosylation. J Biol Chem. 1992; 267:24929–24932. [PubMed: 1281150]

47. McDonald LJ, Moss J. Stimulation by nitric oxide of an NAD linkage to glyceraldehyde-3-phosphate dehydrogenase. Proc Natl Acad Sci U S A. 1993; 90:6238–6241. [PubMed: 8327504]

48. Tao Y, Howlett A, Klein C. Nitric oxide regulation of glyceraldehyde-3-phosphate dehydrogenase activity in Dictyostelium discoideum cells and lysates. Eur J Biochem. 1994; 224:447–454. [PubMed: 7925359]

49. Dell'Antone P. Targets of 3-bromopyruvate, a new, energy depleting, anticancer agent. Med Chem. 2009; 5:491–496. [PubMed: 19534685]

50. Ihrlund LS, Hernlund E, Khan O, et al. 3-Bromopyruvate as inhibitor of tumour cell energy metabolism and chemopotentiator of platinum drugs. Mol Oncol. 2008; 2:94–101. [PubMed: 19383331]

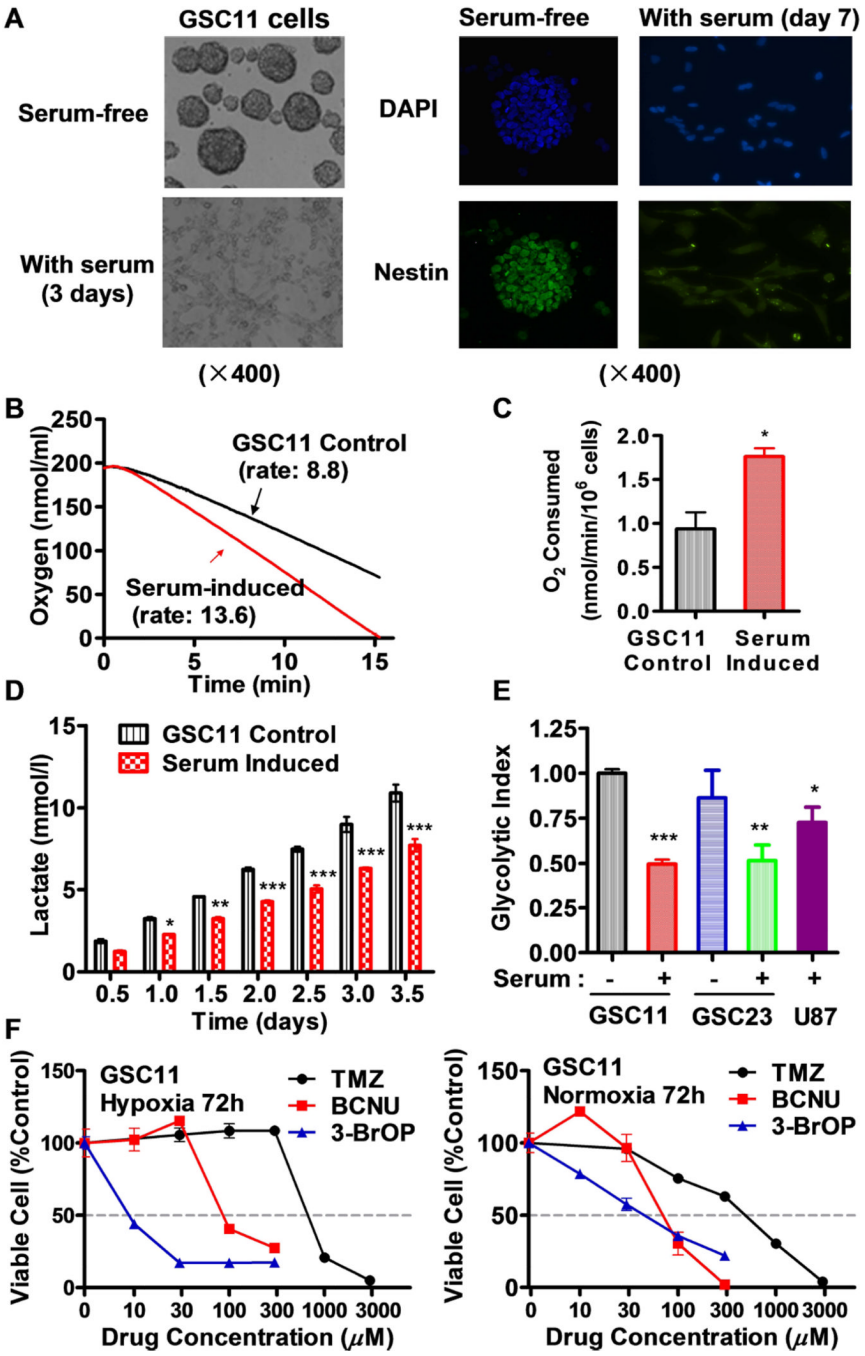

Figure 1.

Low mitochondrial respiration and high glycolysis in glioblastoma stem cells (GSCs) and their resistance to standard chemotherapeutic agents TMZ and BCNU. **(A)** Loss of neurosphere formation and decrease in expression of neural stem cell marker nestin in GSC11 cells after exposure to serum (10% FBS) for the indicated time. **(B)** Representative of mitochondrial respiration rates in GSC11 cells cultured in stem cells medium and in serum-containing medium. Oxygen consumption was measured as an indicator of mitochondrial respiration. **(C)** Quantitative comparison of mitochondrial respiration rates in GSC11 cells cultured in stem cells medium and in serum-containing medium. **(D)** Lactate

generation rates in GSC11 cells maintained in stem cell medium or in serum-containing medium. **(E)** Comparison of glycolytic index in GSC11, serum-induced GSC11, GSC23, serum-induced GSC23 and glioblastoma cell line (U87). Glycolytic index was calculated according to the formula (L × G)/O), in which L is the cellular lactate production, G is the glucose uptake, and O is the oxygen consumption rate. **(F)** Sensitivity of glioblastoma stem cells to TMZ, BCNU, and 3-BrOP under hypoxic and normoxic conditions. GSC11 cells were incubated with the indicated concentrations of drugs for 72 h in normoxia or hypoxia (2% O_2) conditions, and cell viability was measured by MTS assay. *, $p<0.05$; **, $p<0.01$; ***, $p<0.001$.

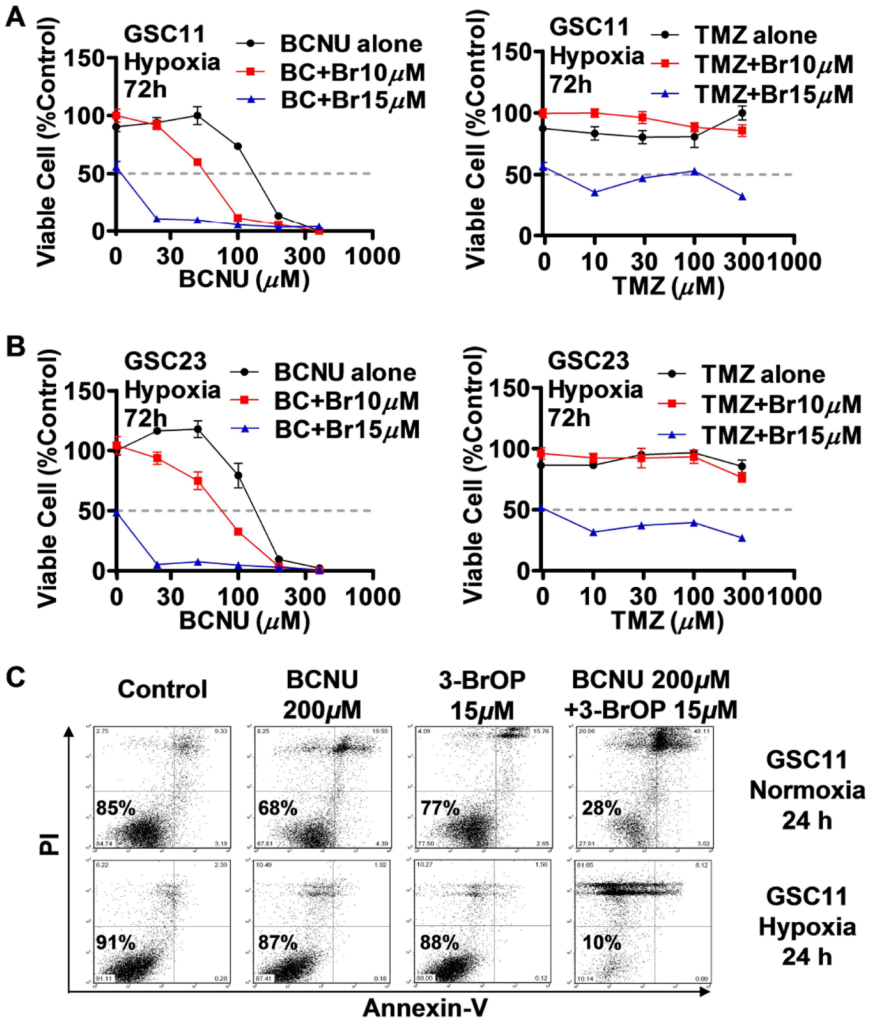

D

Combination Index (CI) of BCNU and 3-BrOP in GSC11

BCNU (μM)	3-BrOP (μM)	CI
100	10	0.979
100	15	0.780
100	20	0.883
200	10	0.701
200	15	0.710
200	20	0.789

Figure 2.

Effective killing of glioblastoma stem cells by combination of 3-BrOP and BCNU. **(A)** Inhibition of GSC11 cells by BCNU (left panel), TMZ (right panel), or their combination with 3-BrOP under hypoxic conditions (2% O_2 for 72 h, MTS assay). **(B)** Inhibition of GSC23 cells by BCNU (left panel), TMZ (right panel), or their combination with 3-BrOP under hypoxic conditions (2% O_2 for 72 h, MTS assay). **(C)** Induction of cell death in GSC11 cells treated with BCNU, 3-BrOP, or their combination. Cells were incubated with the indicated concentrations of compounds for 24 h under normoxic and hypoxic conditions (2% O_2). Cell viability was then measured using annexin-V/PI double staining followed by

flow cytometry analysis. (**D**) Drug combination index (CI) calculated using the Calcusyn software in GSC11 cells treated with BCNU, 3-BrOP alone and in combination for 24 h under hypoxia (2% O_2).

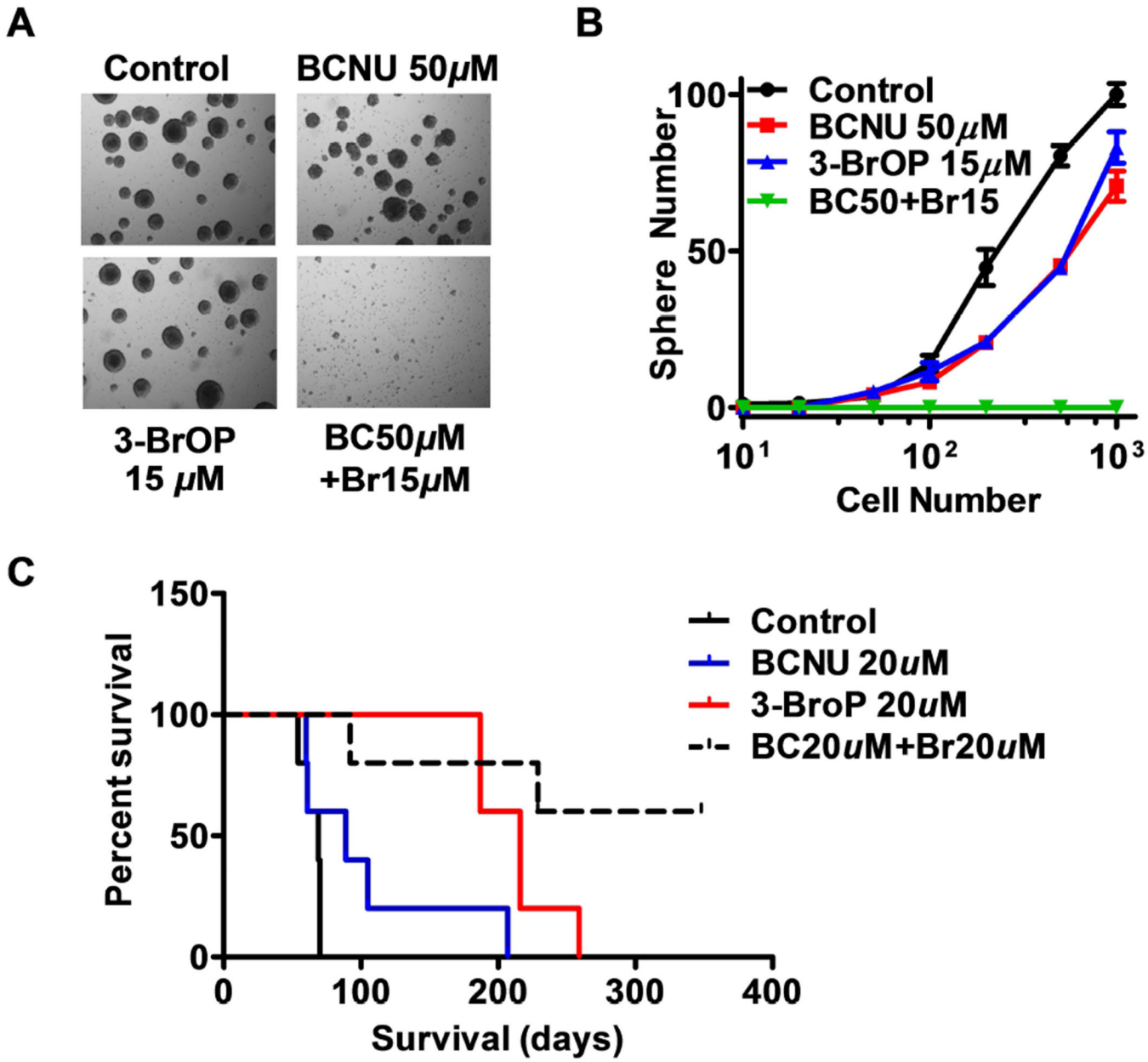

Figure 3.

Impairment on GSC sphere formation in vitro and tumor formation in vivo by combination of 3-BrOP and BCNU. **(A)** Representative morphology of neurosphere formation of glioblastoma stem cells. GSC11 cells were incubated with the indicated concentrations of BCNU, 3-BrOP, or their combination for 3 h, and then cultured in drug-free medium for formation of neurospheres. **(B)** Quantitative data of neurosphere formation in the presence or absence of 3-BrOP and BCNU. **(C)** Effect of 3-BrOP and BCNU on tumor development *in vivo*. GSC11 cells were treated with PBS (control), 20 μM 3-BrOP, 20 μM BCNU, or their combination for 6 h. The cells were then inoculated orthotopically into the brains of mice (5 mice in each group), and mouse survival was monitored (without further drug treatment) as an indication of *in vivo* tumor formation and disease progression.

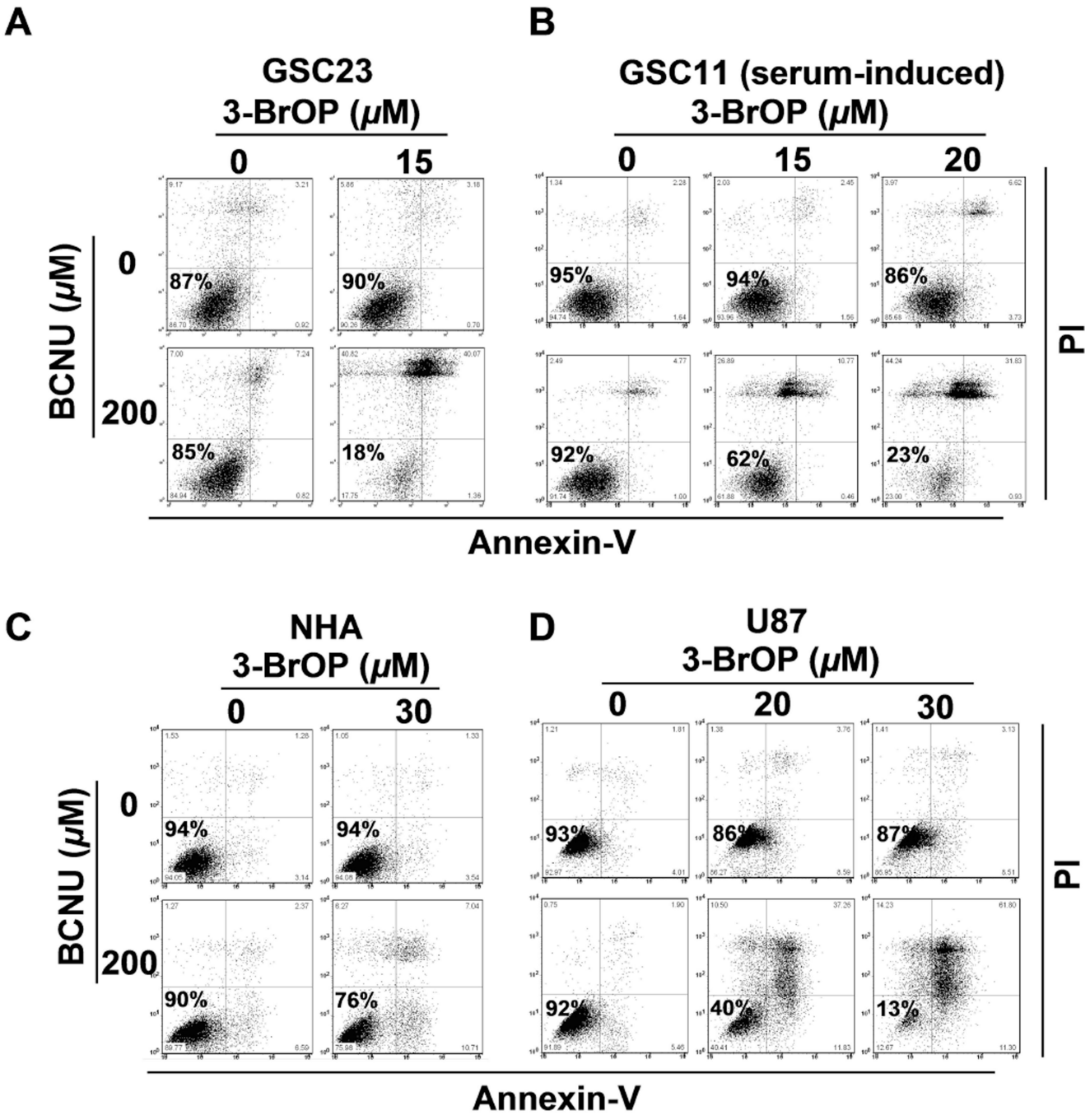

Figure 4.

Preferential killing of glioblastoma cells by 3-BrOP and BCNU. The cytotoxic effects of 3-BrOP, BCNU, or their combination was compared in **(A)** GSC23 cells, **(B)** serum (10% FBS)-induced GSC11 cells, **(C)** non-malignant human astrocytes (NHA), and **(D)** U87 glioma cells. Cells were incubated with the indicated drugs for 24 h under hypoxia (2% O_2), and cell viability was measured by annexin-V/PI double staining followed by flow cytometry analysis.

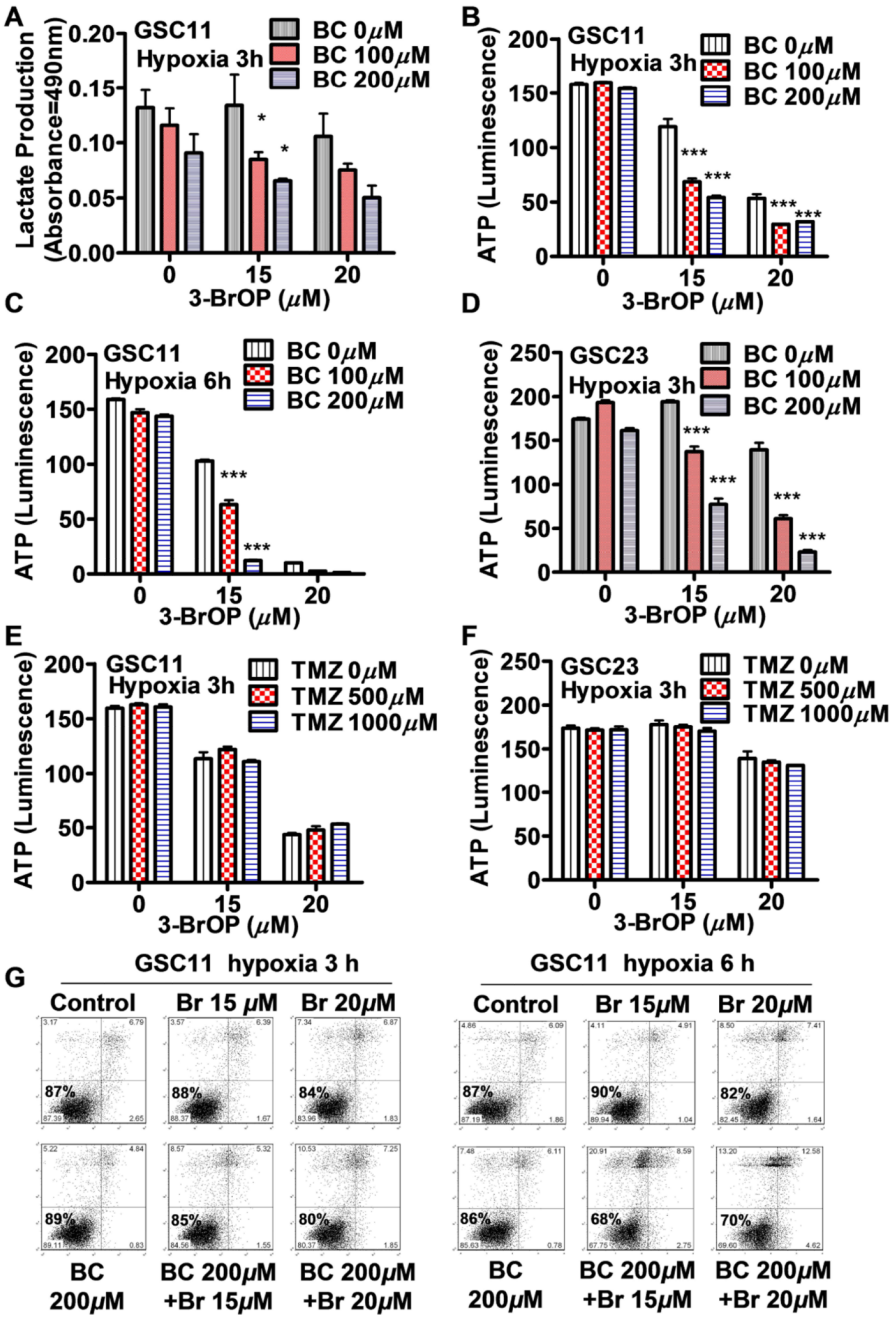

Figure 5.

Effect of 3-BrOP and BCNU or TMZ on energy metabolism in glioblastoma stem cells. **(A)** Inhibition of lactate production in GSC11 cells by the indicated concentrations of BCNU and 3-BrOP under hypoxia (2% O_2). **(B)** ATP depletion in GSC11 cells by the indicated concentrations of BCNU and 3-BrOP for 3 h under hypoxia (2% O_2). **(C)** ATP depletion in GSC11 cells by the indicated concentrations of BCNU and 3-BrOP for 6 h under hypoxia (2% O_2). **(D)** ATP depletion in GSC23 cells by the indicated concentrations of BCNU and 3-BrOP for 3 h under hypoxia. **(E)** ATP depletion in GSC11 cells by the indicated concentrations of TMZ and 3-BrOP for 3 h under hypoxia (2% O_2). **(F)** ATP depletion in

GSC23 cells by the indicated concentrations of TMZ and 3-BrOP for 3 h under hypoxia (2% O_2). **(G)** Viability of GSC11 cells after incubation with 3-BrOP and BCNU for 3 h or 6 h under hypoxic conditions (2% O_2). Cell viability was measured by annexin-V/PI double staining followed by flow cytometry analysis. *, $p<0.05$; ***, $p<0.001$.

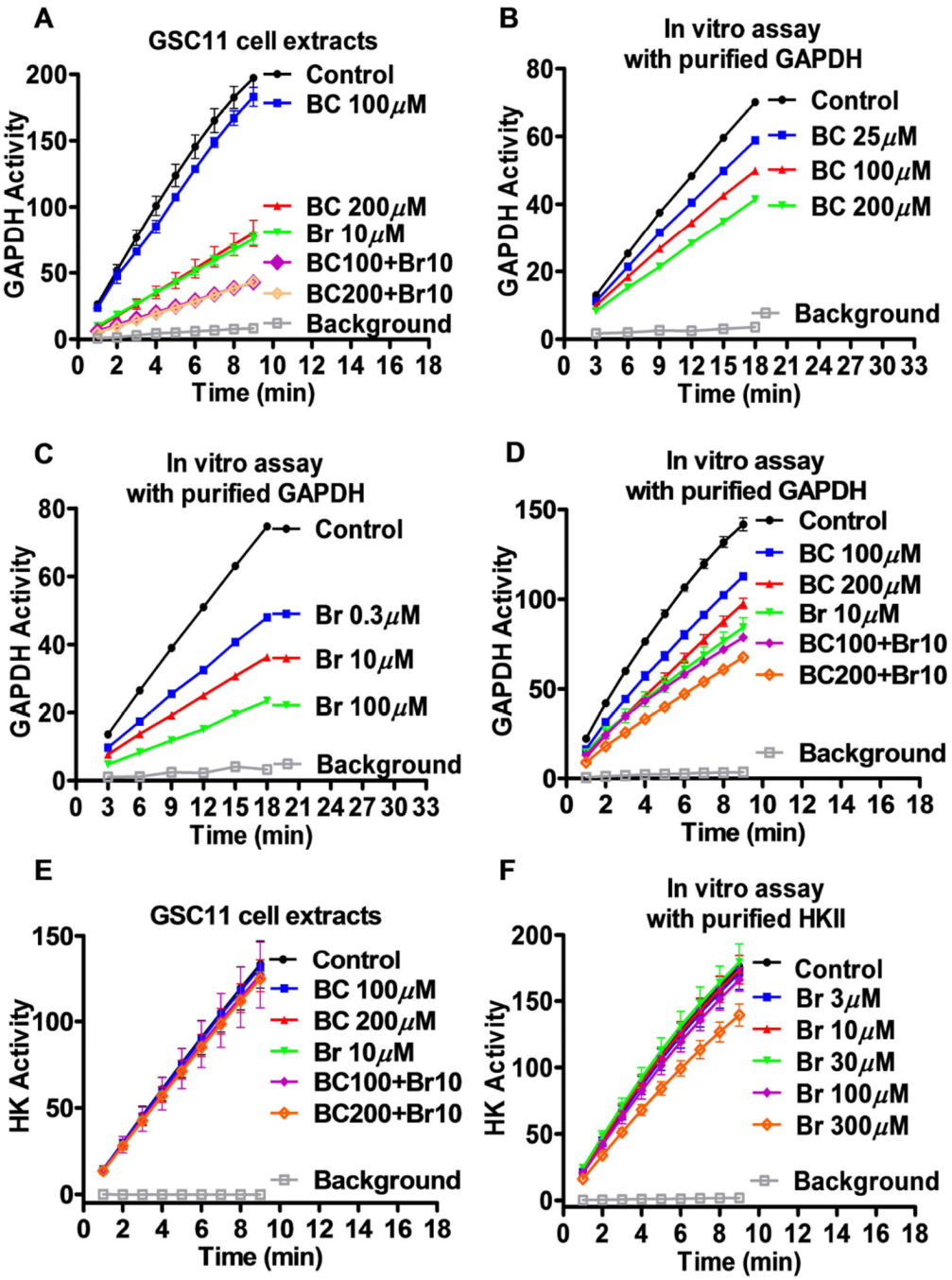

Figure 6.

Inhibition of glyceraldehyde-3-phosphate dehydrogenase (GAPDH) and hexokinase by BCNU and 3-BrOP. **(A)** Effect of BCNU (BC) and 3-BrOP (Br) on GAPDH enzyme activity in GSC11 cells. Cells were first incubated with the indicated concentrations of BCNU or 3-BrOP for 30 min, and protein extracts were prepared for analysis of GAPDH activity without further addition of the compounds *in vitro*. GAPDH activity was measured as described in Materials and Methods. **(B)** Inhibition of purified GAPDH enzyme by BCNU *in vitro*. **(C)** Inhibition of purified GAPDH enzyme by 3-BrOP *in vitro*. **(D)** Inhibition of purified GAPDH enzyme by the combination of BCNU and 3-BrOP *in vitro*.

(**E**) Effect of BCNU, 3-BrOP, or their combination on hexokinase activity in GSC11 cells. Cells were first incubated with the indicated concentrations of compounds for 30 min, and protein extracts were prepared for analysis of hexokinase activity without further addition of the compounds *in vitro*. (**F**) Inhibition of purified hexokinase II enzyme by 3-BrOP *in vitro*.

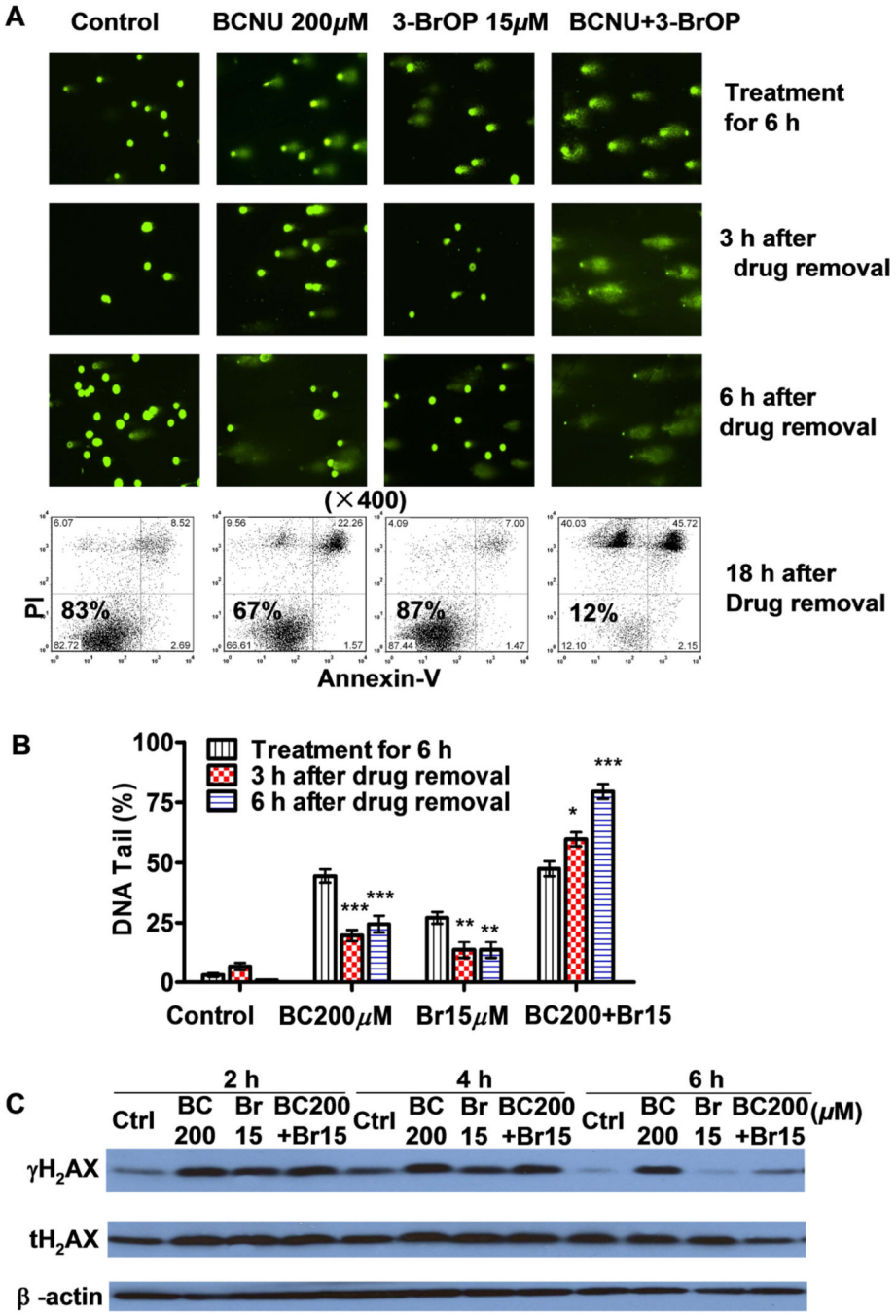

Figure 7.

Effect of 3-BrOP on repair of DNA damage induced by BCNU and cytotoxicity in glioblastome stem cells. **(A)** Comet assay of DNA damage in GSC11 cells treated with BCNU, 3-BrOP, or their combination. Cells were treated with the indicated concentrations of compounds for 6 h, and then either immediately processed for comet assay or cultured in drug-free medium for additional 3–6 h for potential DNA repair. The bright green dots represent the positions of cellular nuclei; the “tail” length and intensity and on the right side of each nucleus represent the degree of DNA strand breaks eluted out from the cell during electrophoresis. Flow cytometry analysis (annexin-V/PI staining) was also used to measure

cell death at 24 h (18 h after drug removal, lower panel). **(B)** Quantification of DNA damage in GSC11 cells treated with or without BCNU and 3-BrOP as indicated. At least 30 cells in each sample were quantitatively analyzed for % of DNA tail that eluted from the cellular nuclei. **(C)** Western blot analysis of γH_2AX and total H_2AX (tH_2AX) proteins in GSC11 cells treated with the indicated compounds for 2–6 h. *, $p<0.05$; **, $p<0.01$; ***, $p<0.001$.